AIP Journal of Applied Physics

Modeling of current gain compression in common emitter mode of a transistor laser above threshold base current

Rikmantra Basu, Bratati Mukhopadhyay, and P. K. Basu

Citation: Journal of Applied Physics **111**, 083103 (2012); doi: 10.1063/1.4703926
View online: http://dx.doi.org/10.1063/1.4703926
View Table of Contents: http://scitation.aip.org/content/aip/journal/jap/111/8?ver=pdfcov
Published by the AIP Publishing

JOURNAL OF APPLIED PHYSICS **111**, 083103 (2012)

Modeling of current gain compression in common emitter mode of a transistor laser above threshold base current

Rikmantra Basu,[1,2,a)] Bratati Mukhopadhyay,[1,b)] and P. K. Basu[1,c)]
[1]*Institute of Radio Physics and Electronics, University of Calcutta, 92 Acharya Prafulla Chandra Road, Kolkata 700 009, India*
[2]*Centre for Research in Nanoscience and Nanotechnology, University of Calcutta, JD Block, Sector III, Salt Lake, Kolkata 700 106, India*

(Received 31 January 2012; accepted 13 March 2012; published online 18 April 2012)

We have obtained the expressions for the terminal currents in a heterojunction bipolar transistor laser the base of which contains a quantum well (QW). The emitter-base junction is assumed to be abrupt, leading to abrupt discontinuity in quasi-Fermi level at the interface. The expressions for the terminal currents as a function of collector-emitter and base-emitter voltages are obtained from the solution of the continuity equation. The current density in the QW located at an arbitrary position in the base is related to the virtual state current density. The threshold current density in the QW is calculated by using the expression for gain obtained from Fermi golden rule. The plot of collector current (I_C) versus collector-emitter voltage (V_{CE}) for different values of base current shows the usual transistor characteristics, i.e., a rising portion after a cut-in V_{CE}, and then a saturation behavior. The dc current gain remains constant. However, as the base current exceeds the threshold, a stimulated recombination rate is added to the spontaneous recombination rate and the plots of collector currents become closer for the same increase in base current. This current gain compression is in agreement with the experimental observation. Our calculated values qualitatively agree with other experimental findings; however some features like Early effect do not show up in the calculation. © *2012 American Institute of Physics*. [http://dx.doi.org/10.1063/1.4703926]

I. INTRODUCTION

Transistor laser (TL) has the unique feature of working as both an electronic and a photonic device. Basically it is a heterojunction bipolar transistor (HBT) in which the emitter and collector terminals are used for electrical signal input and output, respectively. For sufficient injection of carriers into the base, which incorporates a quantum well (QW), population inversion occurs between the electron and hole subbands in the QW. With the base current exceeding a threshold value, the optical gain in the QW overcomes the sum of the material and mirror losses, leading to the emission of coherent light in a direction perpendicular to that of the current flow.

The first laser action from HBT was observed by Feng and co-workers[1,2] and to date, most of the experimental reports on TL have come from their group. The workers have mostly considered InGaP–GaAs–GaAs HBTs with InGaAs QW in the base,[1–3] in addition to other material combinations,[4,5] and type II heterostructures[6]. They reported[7] emission at 1554 nm, the wavelength for fiber optic communication. Electrical-optical signal mixing and multiplication using tunnel junctions were also reported.[8] The authors studied in detail modulation bandwidth[9,10] and even reported resonance free frequency response.[11] They also reported analytical results on the charge distribution in the base by using experimental I-V characteristics and charge control model for transistors[12] and presented a microwave circuit model for the TL.[13]

Analytical modeling of the heterojunction bipolar transistor laser (HBTL) has also been presented recently by different groups. Zhang and Leburton[14] proposed an analytical model by relying on the rate equations for both the carriers and photons. To obtain the rate equations for the carrier numbers in the QW, they introduced a capture coefficient expressed in terms of the thickness of the base and the QW and capture lifetime by the QW.

Faraji *et al.*[15–17] solved the continuity equation in the base in the presence of diffusion and recombination[18] to obtain the charge distribution. They used the concept of virtual state (VS) to relate the bulk carriers with the two-dimensional (2D) carriers, as the recombination in the QW occurs between the quantized energy levels in the QW. They also considered capture of carriers by, as well as their escape from, the QW. In their work, however, the QW was assumed to be placed at the middle of the base region, whereas in actual experiments the QWs are placed nearer to the base-collector junction.[2,9,12,13] Further, the charge distribution profile obtained in their work does not show a break at the position of the QW in disagreement with the experimental findings. A more general analytical model is proposed by Basu *et al.*[19,20] considering an arbitrary position of the QW in the base region, gain in QW with 2D density-of-states, Fermi's "golden rule," and broadening of states. In this model, the value of threshold base current, light power output, and the charge carrier distribution profile agree satisfactorily with the results as given by Feng and co-workers.[12,13]

As TL is a transistor, its electrical input and output characteristics resemble those of a normal transistor. For example, in the common emitter (CE) mode of operation in the

[a)]Electronic mail: rikmantra@gmail.com.
[b)]Electronic mail: bmrp@caluniv.ac.in.
[c)]UGC-BSR Faculty Fellow. Electronic mail: pkb.rpe@caluniv.ac.in.

active region, the output characteristics consist of a family of curves showing variation of collector current (I_C) with collector-emitter voltage (V_{CE}) with base current I_B as the parameter. Such output characteristics have been obtained by Feng *et al*. in a number of publications. A noteworthy feature of the characteristics is that the I_C curves in the saturation region (or slightly rising part showing Early effect) become congested once I_B exceeds the threshold base current I_{Bth}. In other words, the dc (also ac) gain reduces once I_{Bth} is exceeded. This is called gain (β) compression. Unfortunately however, none of the theories mentioned previously, including our own, which successfully explained a number of experimental findings, are suitable to calculate the output characteristics and demonstrate β-compression.

In view of this, we feel motivated to develop a more general analytical model that can give terminal currents from "contact to contact." In this context, it is extremely necessary to make a detailed study of transport across the heterointerface, which may be a graded gap or an abrupt type where the general drift-diffusion expression is not valid due to the discontinuity in the quasi-Fermi levels (alternately termed as imref in some publications, e.g., in Ref. 21) at the heterointerface. Grinberg and Luryi[21] reported a detailed theory of the minority carrier transport in HBT with a particular emphasis on the difference between the cases of abrupt and graded emitter-base junctions and the role in the former case of the quasi-Fermi level (imref) discontinuity at the interface. In this paper, we have considered an HBTL with abrupt E-B junction with a QW placed in an arbitrary position in the base region and developed the expressions for terminal currents considering the concept of VS, as well as the discontinuity in the quasi-Fermi level at the abrupt emitter-base junction. The nature of variation of the collector current is in agreement with the experimental findings[12,13] and shows gain compression above the threshold base current.

The present paper is organized as follows: Sec. II gives the detailed theory of discontinuity of the quasi-Fermi level at the abrupt junction; in Sec. III the expressions for the terminal currents are developed. This section also outlines the calculation of optical gain and threshold and the way to include stimulated recombination. The method of calculation is briefly outlined in Sec. IV. The calculated results are presented and discussed in light of experimental data in Sec V. Section VI concludes our work.

II. THEORY OF DISCONTINUITY OF QUASI-FERMI LEVEL AT THE ABRUPT JUNCTION

The structure considered in this paper is an HBT with higher bandgap n-type InGaP emitter (E) layer, p-type GaAs base (B) layer with an InGaAs QW embedded in it and an n-type GaAs collector (C) layer. In this structure, the emitter-base junction is taken to be abrupt, whereas the collector-base junction is taken to be a graded one. The coordinate of the position of the E-B junction is taken at $x = 0$, W is the base width and x_1 is the coordinate of the center of the QW as shown in Fig. 1.

The theory is developed following the method of Grinberg and Luryi.[21] Here the base width W is considered sufficiently larger than the characteristic scattering length ($l_{sc} = D/v_T$), where D is the diffusion coefficient and v_T is the thermal velocity of the minority carriers.

The basic relationships used here are

$$\int_{c_1}^{c_2} \frac{J_n dx}{\mu n} = eV \tag{1}$$

and

$$np = n_i^2 e^{eV/kT}, \tag{2}$$

where J_n is the electron current density, V is the applied bias, $\mu = eD/kT$ is the electron mobility, n and p are the electron and hole concentrations, n_i is the intrinsic carrier concentration, c_1 is the emitter contact and c_2 is the auxiliary contact deep in the base.

Although both Eqs. (1) and (2) do not implicitly rely on the discontinuity of the quasi-Fermi level (imref), there is indeed a discontinuity of the quasi-Fermi level E_{fn} for electrons in the vicinity of the abrupt interface at the emitter-base junction. Therefore, the first integral will be a sum of integrals as, $\int_{c_1}^{-\varepsilon}$ and $\int_{+\varepsilon}^{c_2}$ excluding a small region, ε, around the junction interface in which a finite drop of quasi-Fermi level variation, $\delta E_{fn} = E_{fn}(+\varepsilon) - E_{fn}(-\varepsilon)$, occurs. The transport in this region is governed by thermionic emission.

The quasi-Fermi level E_{fn} in a graded gap semiconductor is given by

$$E_{fn} = E_c + kTln(n/N_C), \tag{3a}$$

whereas the jump in the quasi-Fermi level at the abrupt interface is

$$\delta E_{fn} = \Delta - kTln\left(\frac{n^+ N_C^{(E)}}{n^- N_C^{(B)}}\right) = kTln\left(1 - \frac{J_n e^{\Delta/kT}}{en^+ v_R}\right), \tag{3b}$$

where Δ is the conduction band discontinuity, n^+ and n^- are the electron concentrations in the base near the emitter

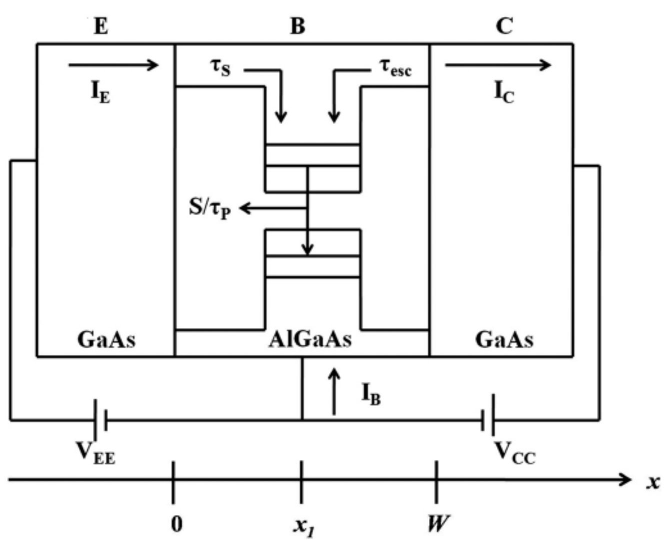

FIG. 1. Schematic diagram of HBTL.

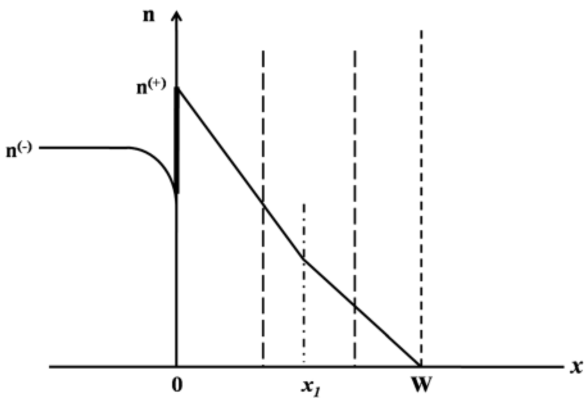

FIG. 2. Schematic of electron concentration profile.

junction and on the emitter side of the abrupt junction, respectively, as shown in Fig. 2. $N_C^{(E)}$ and $N_C^{(B)}$ are the conduction band density of states in the emitter and base, respectively, in the vicinity of the discontinuity. v_R is the Richardson velocity given by $v_R = \sqrt{kT/2\pi m}$, with m as the effective mass of electrons in the base. The conduction band edge $E_c = -e(\phi+\chi)$ results from the electrostatic potential ϕ and the variable affinity χ.

So the current relationship becomes

$$\frac{J_n}{e\mu n} = -\frac{d(\phi+\chi)}{dx} + \frac{kT}{e}\frac{d}{dx} ln\left(\frac{n}{N_C}\right). \tag{4}$$

Now, integrating Eq. (4) over any region including the band discontinuity (at $x=0$) and by excluding the infinitesimal region ε near the origin,

$$\int_{c_1}^{c_2} \frac{J_n dx}{e\mu n} = \int_{c_1}^{-\varepsilon} \frac{J_n dx}{e\mu n} + \int_{+\varepsilon}^{c_2} \frac{J_n dx}{e\mu n}. \tag{5}$$

Thus, substituting Eq. (4) into Eq. (5), we get

$$\int_{c_1}^{-\varepsilon} \frac{J_n dx}{\mu n} + \int_{+\varepsilon}^{c_2} \frac{J_n dx}{\mu n} = eV - \Delta + kTln\left(\frac{n^+ N_C^{(E)}}{n^- N_C^{(B)}}\right)$$
$$= eV - \delta E_{fn} \tag{6}$$

with $n^+ p^+ [N_C^{(B)}/N_C^{(E)}](n^-/n^+) e^{\Delta/kT} = n_i^2 e^{eV/kT}$ and δE_{fn} as given in Eq. (3b).

The actual value of n^-/n^+ will be determined from the boundary conditions of the electronic flux as

$$-\frac{J_n}{e} = v_R N_C^{(B)} \left[\frac{n^-}{N_C^{(E)}} - \frac{n^+}{N_C^{(B)}} e^{-\Delta/kT}\right] \tag{7}$$

or

$$\frac{n^+ N_C^{(E)}}{n^- N_C^{(B)}} = 1 - \frac{J_n e^{\Delta/kT}}{e v_R n^+}. \tag{8}$$

Using the previous equations we get

$$\delta E_{fn} = \Delta - kTln\left(\frac{n^+ N_C^{(E)}}{n^- N_C^{(B)}}\right) = kTln\left(1 - \frac{J_n e^{\Delta/kT}}{en^+ v_R}\right). \tag{9}$$

Here, we assume that strong forward and reverse biases are applied to the emitter-base junction and the collector-base junction, respectively, and therefore we may write to a good approximation $J_n \approx -eDn^+/W$, and from Eq. (9),

$$\delta E_{fn} = kTln\left(1 + \frac{De^{\Delta/kT}}{Wv_R}\right), \tag{10}$$

where W is the base width. If the simplest model of collisions in the base is considered where scattering length l_{sc} is independent of electron energy, then, $D = 4v_R l_{sc}/3$. Thus, from Eq. (10) we get

$$\delta E_{fn} = kTln\left(1 + \frac{4l_{sc} e^{\Delta/kT}}{3W}\right). \tag{11}$$

To obtain a more general solution, we consider a forward biased *n-p* heterojunction with non-negligible base depletion $(N_D \le N_A)$. If we let $n(0) = n^+ e^{-e\delta\phi/kT}$, where $\delta\phi$ is the electrostatic potential drop on the base side of the junction and is given by

$$\delta\phi = \frac{(\phi_0 - V)\varepsilon_E N_D}{\varepsilon_E N_D + \varepsilon_B N_A}, \tag{12}$$

with ϕ_0 as the built-in-potential and ε_E and ε_B, the permittivities of emitter and base sides, respectively, then from Eqs. (8) and (12), we get

$$\delta E_{fn} = kTln\left(1 + \frac{De^{(\Delta - e\delta\phi)/kT}}{Wv_R}\right). \tag{13}$$

If we now consider the recombination on the base with the diffusion length of electrons in the base as L_D, the discontinuity in the quasi-Fermi level becomes

$$\delta E_{fn} = 1 + \frac{De^{(\Delta - e\delta\phi)/kT}}{L_D v_R tanh(W/L_D)}. \tag{14}$$

Energy band diagram of the structure under bias is shown in Fig. 3.

III. EVALUATION OF TERMINAL CURRENTS AND OPTICAL GAIN

In our following calculations, as $m_e = 0.063\mathrm{m}_0$ and $D = 26\ \mathrm{cm}^2\ \mathrm{s}^{-1}$, the length D/v_T is 5.6 nm, which is very small compared to the base width ~100 nm. Further, under low level injection from the emitter to the base by thermionic emission and tunneling, the carriers occupy energy levels very close to the conduction band edge, so they thermalize. In addition, the electric field in the base being very small, the transport is almost dominated by diffusion.[21]

The time-independent continuity equation for diffusion dominated transport is given by

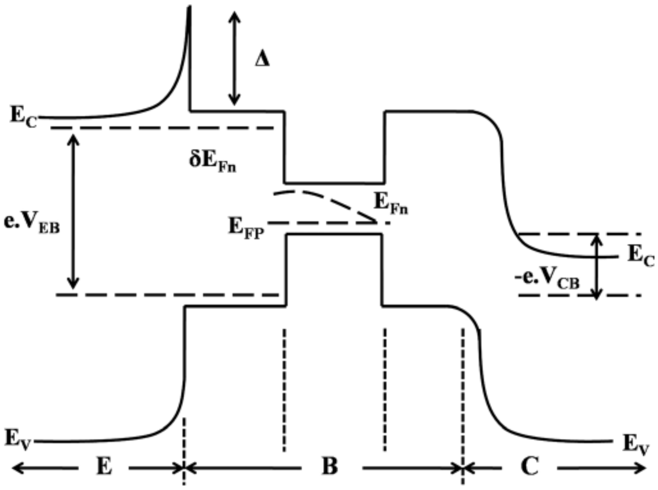

FIG. 3. Energy band diagram of HBTL under bias.

$$\frac{\partial^2 n}{\partial x^2} = \frac{n - n_0}{L_D^2}, \tag{15}$$

where $(n - n_0)$ is the excess electron density with n_0 as the initial electron density at equilibrium and L_D is the diffusion length.

The solution of the previous equation is as follows:

$$n - n_0 = C_1 e^{x/L_D} + C_2 e^{-x/L_D}. \tag{16}$$

A. Emitter current

To evaluate the emitter current, the boundary conditions are as follows. At $x = 0$, $eD(\partial/\partial x)(n - n_0) = J_E$; $x = x_1$, $n - n_0 = N_{vs} - n_0$; and $x = W$, $n - n_0 = n_w - n_0$, where N_{vs} is the VS carrier density and $n(W) = n_w$. Applying the above-mentioned boundary conditions to Eq. (16), we obtain the carrier concentration before and after the QW as

$$\delta N_1(x) = \frac{(N_{vs} - n_0) + (J_E L_D/eD)e^{-z_1}}{2\,cosh(z_1)} e^{x/L_D} + \frac{(N_{vs} - n_0) - (J_E L_D/eD)e^{z_1}}{2\,cosh(z_1)} e^{-x/L_D}, \tag{17a}$$

$$\delta N_2(x) = \frac{(n_w - n_0)e^{-z_1} - (N_{vs} - n_0)e^{-W/L_D}}{2\,sinh(z_2)} e^{x/L_D} + \frac{(N_{vs} - n_0)e^{W/L_D} - (n_w - n_0)e^{z_1}}{2\,sinh(z_2)} e^{-x/L_D}, \tag{17b}$$

where $z_1 = x_1/L_D$, $z_2 = W - x_1/L_D$, and the corresponding virtual current density is

$$J_{vs} = eD\left[\frac{\partial}{\partial x}(\delta N_1)_{x_1^+} - \frac{\partial}{\partial x}(\delta N_2)_{x_1^-}\right].$$

From the previous three equations we obtain the expression for emitter current as

$$J_E = J_{vs} cosh(z_1) - \frac{eD}{L_D}(N_{vs} - n_0)[sinh(z_1) + coth(z_2)cosh(z_1)] + \frac{eD}{L_D}\frac{(n_w - n_0)cosh(z_1)}{sinh(z_2)}. \tag{18}$$

As the carriers entering the VS have two possibilities, falling in the QW states or diffusing to the collector, the steady state equation of the VS carrier concentration is given by

$$\frac{J_{vs}}{ed} = \frac{J_{QW}}{ed} + \frac{N_{vs}}{\tau_s}, \tag{19}$$

where τ_s is the spontaneous lifetime of the carrier.

Again, the VS carriers are linked to the QW 2D carriers by the relation

$$\frac{J_{QW}}{ed} = \frac{N_{vs}}{\tau_{cap}} - \frac{N_{QW}}{\tau_{esc}}, \tag{20}$$

where τ_{cap} is the carrier lifetime for the carriers falling from the VS to the QW 2D states and τ_{esc} is the escape lifetime from the QW 2D states to the VS. We have neglected the escape phenomena of the carriers from the QW in our following calculations.

Using the previous relations we can write the emitter current from Eq. (18) as

$$J_E = (A - B)(N_{vs} - n_0) + C(n_w - n_0), \tag{21}$$

where $A = eD(1/\tau_{cap} + 1/\tau_s)cosh(z_1)$, $B = (eD/L_D)[sinh(z_1) + cosh(z_1)coth(z_2)]$, and $C = (eD/L_D)[cosh(z_1)/sinh(z_2)]$.

Now, from the concept of discontinuity of quasi-Fermi level, we know

$$n^+ - n_0 = n_0(e^{eV_{EB}/kT} - 1) + \frac{J_E e^{\Delta/kT}}{ev_R},$$
$$n_w - n_0 = n_0(e^{eV_{CB}/kT} - 1),$$

where V_{EB} and V_{CB} are the emitter-base and collector-base voltages, respectively. Again $(n^+ - n_0)$ can be related to $\delta N_1(x)$ by the relation $(\partial/\partial x)(\delta N_1)|_{x=0} = n^+ - n_0$.

So finally, the emitter current comes out as

$$J_E = \alpha F_{EB} + \xi F_{CB}/(\gamma - \beta - \sigma), \tag{22}$$

where $F_{EB} = e^{eV_{EB}/kT} - 1$, $F_{CB} = e^{eV_{CB}/kT} - 1$, $\alpha = n_0 cosh(x_1/L_D)$, $\beta = (e^{\Delta/kT}/ev_R)cosh(x_1/L_D)$, $\gamma = 1/(A - B)$, $\xi = Cn_0\gamma$, and $\sigma = (L_D/eD)sinh(z_1)$.

B. Collector current

In this case, the boundary conditions are

At $x = x_1$, $n - n_0 = N_{vs} - n_0$, and at $x = W$, $eD(\partial/\partial x)(n - n_0) = J_C$.

Applying the same procedure as explained previously, the collector current is obtained as

$$J_C = \eta(N_{vs} - n_0) + J_E(N_{vs} - n_0)\theta\lambda - J_{vs}cosh(z_2), \tag{23}$$

where $\eta = (eD/L_D)cosh(z_2)$, $\theta = (eD/L_D)sinh(z_2)$, and $\lambda = cosh(z_2)/cosh(z_1)$. Finally, the base current is calculated using the following fundamental relation:

$$J_B = J_E - J_C. \tag{24}$$

C. Optical gain

The relationship between threshold current density in the QW and the threshold base current density with the VS as the intermediary has been developed in our earlier publications.[19,20] We give here the essential features. The expression for gain using **k**-conservation in 2D ($\mathbf{k}_t$ and $\mathbf{r}_t$ are, respectively, the 2D wave vector and the position vector), Fermi functions *f* and Lorentzian line shape function is[19,22]

$$g(\hbar\omega) = C_0 \sum_{n,m} \left|I_{h,m}^{c,n}\right|^2 \int_0^\infty dE_t \rho_r^{2D} \left|\hat{e}\cdot p_{cv}\right|^2 \times \frac{\gamma/(2\pi)}{\left(E_{h,m}^{c,n}(\mathbf{k}_t) - \hbar\omega\right)^2 + (\gamma/2)^2}\left[f_c^n(E_t) - f_v^m(E_t)\right], \tag{25}$$

where

$$C_0 = \frac{\pi q^2}{n_r c \varepsilon_0 m_0^2 \omega}, \rho_r^{2D} = \frac{m_r}{\pi\hbar^2 d}, \quad I_{hm}^{cn} = \int_{-\infty}^{\infty} dx \phi_n(x) g_m(x),$$

where ρ_r^{2D} is the reduced density-of-states function for 2D for quantized motion along the *x*-direction, *d* being the width of the QW, *I* stands for the overlap of envelope functions for electron (in the *n*th subband) and hole (in the *m*th subband), $\hbar\omega$ is the photon energy, $|\hat{e}\cdot p_{cv}|^2$ is the momentum matrix element for QWs, and γ is the finite linewidth of the spectrum. In Eq. (25), *c* is the speed of light in free space, ε_0 is the permittivity of free space, n_r is the background refractive index, and m_0 is the free electron mass. The kinetic energy for 2D free motion, E_t, is considered to be zero for the band edge transition. The Fermi occupation probabilities are expressed in terms of quasi-Fermi levels F_c and F_v.

From the plots of gain or absorption spectra for various injected carrier densities the values of maximum gain, the value of *a:* the differential gain constant and of N_{tr}, the transparency carrier density are obtained. Knowing the value of current density at transparency via the relation $J_r = qdN_{tr}/\tau_s$, the threshold current density is obtained from $J_{th} = J_{tr} + [qd/\Gamma\eta a\tau_s][\alpha + (1/2L)ln(1/R_1R_2)]$, where Γ is the optical confinement factor, η is the internal quantum efficiency, α is the loss coefficient, *L* is the length of the device, and R_1 and R_2 are the respective reflectivities of the front and the back mirrors.

The stimulated emission provides another recombination channel in the QW. The overall effect is to replace the recombination lifetime τ_S by an effective lifetime defined as follows:

$$\tau^{-1} = \tau_S^{-1} + \Gamma v_g g N_p, \tag{26}$$

where $N_p = \eta(I_B - I_{Bth})/(qv_g\alpha_m)$ per unit area. Here, η is the internal quantum efficiency, v_g is the group velocity, and α_m is the mirror loss.

IV. CALCULATION METHODOLOGY

We considered the device dimensions and time constants as given by Feng *et al.*[12] Here the base of the TL is treated as a series of three regions: 510 Å of GaAs doped to a level of 10^{19}/cm^3, a 160 Å undoped InGaAs QW, and 210 Å of GaAs with doping density of 10^{19}/cm^3. The values of other parameters used in the calculation are entered in Table I. First of all we have calculated the threshold base current following the method of Basu *et al.*[19] and obtained the threshold base current as 21.6 mA. We next attempt to calculate the collector currents for different base currents. For this purpose, we first calculate the emitter current with Eq. (22), where a fixed value of V_{EB} is considered to make the base current constant, whereas V_{CB} is varied to obtain a variation in V_{CE} $(= V_{EB} - V_{CB})$. Here the discontinuity in the quasi-Fermi level has been taken into consideration. The value of the VS carrier density N_{VS} due to a particular value of the emitter current can easily be calculated using Eq. (21). Again for this particular value of N_{VS}, the VS current density is evaluated with Eqs. (19) and (20). Although N_{VS} and J_{VS} are known, it is easy to calculate the collector current and base current using Eqs. (23) and (24).

In Eq. (19), the VS carrier concentration, VS current density, and QW current are related via spontaneous carrier lifetime. It is to be mentioned here that, when the base current is below the threshold value, only spontaneous emission occurs. But above the threshold base current, both spontaneous and stimulated emission occurs, and in Eq. (19) spontaneous emission lifetime is modified accordingly.

V. RESULTS AND DISCUSSIONS

The values of parameters used in the calculation are entered in Table I. We have obtained the plots of $\delta N_1(x)$ and $\delta N_2(x)$ as given by Eqs. (17a) and (17b) for an InGaAs QW placed 59 nm away from the EB junction in a GaAs base of

TABLE I. Values of parameters used in calculation.

Electron capture lifetime, τ_{cap}	10 ps	Escape lifetime, τ_{esc}	1.5 ps
Spontaneous emission time, τ_s	200 ps	Photon lifetime, τ_p	4 ps
Base recombination lifetime, τ_B	193 ps	Diffusion coefficient, D_n	26×10^{-4} m^2/s
Group velocity, ν_g	8.67×10^7 m/s	Loss coefficient/unit length, α	500 m^{-1}
Confinement factor, Γ	0.03	Richardson velocity, V_R	10^5

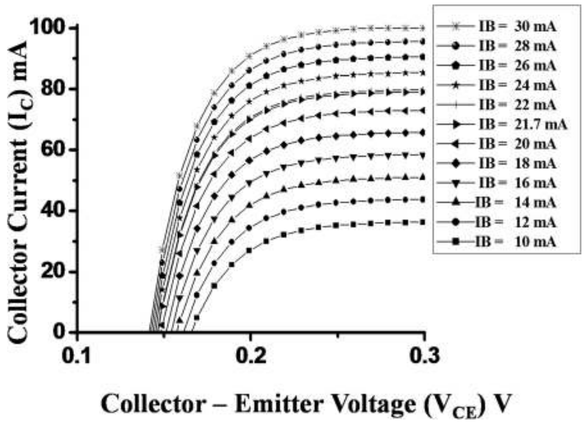

FIG. 4. Variation of collector current as a function of collector-emitter voltage for different injected base currents [$I_B = 10$ mA (square); 12 mA (circle); 14 mA (triangle); 16 mA (inverted triangle); 18 mA (diamond); 20 mA (left-pointing triangle); 21.7 mA (right-pointing triangle); 22 mA (plus sign); 24 mA (star); 26 mA (pentagon); 28 mA (oval); and 30 mA (asterisk)].

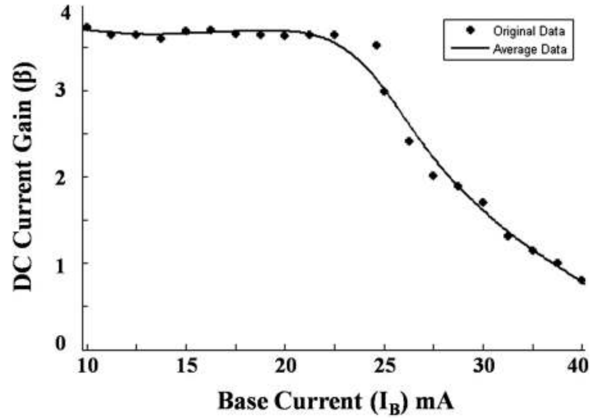

FIG. 5. Variation of dc current gain as a function of base current.

width ~88 nm. The plots are straight lines with different slopes and the break occurs at the location of the QW. This nature of charge variation and the calculated I_{Bth} of 21.6 mA are in complete agreement with the experimental data.[12] Details of this work are given in earlier publications.[19,20]

In the present work, our primary aim is to obtain the family of collector currents for a common-emitter mode of operation. Our calculated values of collector current for different values of collector-emitter voltage (V_{CE}) with a base current as a parameter are shown in Fig. 4. For different base-emitter voltages as parameters, corresponding collector-emitter voltages are first estimated. Next the quasi-Fermi levels (or imref) discontinuities are calculated and with the help of those values terminal currents are evaluated using Eqs. (18)–(24). The family of curves is almost identical with the family for normal transistors. After a cut-in value the collector current rises and then shows saturation behavior. It is interesting to note that for base currents smaller than the threshold base current (21.6 mA in this structure) the spacing between adjacent characteristic curves is almost constant. However, as the base current exceeds the threshold value the collector current curves get closer for the same increment of the base current. This phenomenon is known as β-compression, which has already been demonstrated in experiments.[9,12,13] This phenomenon is not observed in normal transistors for which all the characteristic curves are almost equally spaced. This occurs due to the onset of a stimulated recombination process in the QW above threshold.

To further illustrate the β-compression above threshold base current we have shown the variation of dc current gain with injected base current in Fig. 5, which clearly shows the β-compression as the base current increases beyond threshold.

We note at this point that the β-compression, as displayed in Figs. 4 and 5, has already been demonstrated by Feng and co-workers in a number of publications. Our calculation corroborates their experimental findings.

The variation of effective emission lifetime with injected base current starting from threshold is plotted in Fig. 6 as it gets modified above threshold, according to Eq. (26). Beyond the lasing threshold effective emission lifetime decreases as stimulated emission speeds up the overall rate of recombination in the base region.

It is now of interest to examine quantitative agreement between our calculated values and the experimental data. We first note from Fig. 4 that our cut-in value of V_{CE} is ~0.15 V, whereas the value in experiments[12,13] is ~0.3 V. It is to be noted that Then *et al.* in their microwave circuit model[13] indicated the presence of three series resistances belonging to the three terminals. In our work, we did not consider their existence. Therefore, our V_{CE} values are intrinsic, whereas in the experiments the value is between external leads. The calculated collector current at I_{Bth} is ~3 times too high than the value in experiment. Consequently our values of dc gain drops from 4 to 2 once I_{Bth} is exceeded. In the experiments however the β-compression is less drastic.

Our present model cannot account for the usual Early effect exhibited by HBTs as well as by HBTLs. We feel that a refined theory relying on the Gummel-Poon model may be needed for this purpose. However, it is not clear at this stage if such a refined theory would lead to an analytical solution of the problem.

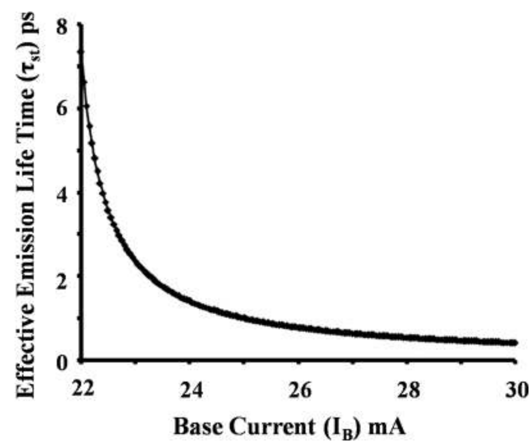

FIG. 6. Variation of effective emission lifetime as a function of base current.

VI. CONCLUSIONS

In the present study, the terminal currents in an HBTL incorporating a QW in the base are expressed in terms of terminal voltages V_{CE} and V_{BE}. The expressions differ from those for normal HBTs as a large fraction of the injected base current is responsible for light emission in the QW. A thermionic diffusion model developed by Grinberg and Luryi is employed to find the discontinuity of quasi-Fermi level at the EB heterointerface.

The calculated threshold base current in the present model agrees very well with experimental value. The nature of collector current variation in the common emitter mode of operation is similar to the behavior of normal transistors below the threshold base current. Above this threshold, the collector current curves are closer in conformity with experimentally observed gain compression in complete agreement with experiment. However, the calculated values of collector current and the dc gain are somewhat higher than in experiments, which may be due to series resistance effects. Our calculated characteristics do not show the Early effect and therefore a refined theory may be needed.

[1]N. Holonyak, Jr. and M. Feng, IEEE Spectrum. **43**, 50 (2006).
[2]G. Walter, N. Holonyak, Jr., M. Feng, and R. Chan, Appl. Phys. Lett. **85**, 4768 (2004).
[3]M. Feng, N. Holonyak, Jr., G. Walter, and R. Chan, Appl. Phys. Lett. **87**, 131103 (2005).
[4]F. Dixon, R. Chan, G. Walter, N. Holonyak, Jr., M. Feng, X. B. Zhang, J. H. Ryou, and R. D. Dupuis, Appl. Phys. Lett. **88**, 012108 (2006).
[5]B. F. Chu-Kung, M. Feng, G. Walter, N. Holonyak, Jr., T. Chung, J. H. Ryou, and R. D. Dupuis, Appl. Phys. Lett. **89**, 082108 (2006).
[6]M. Feng, N. Holonyak, Jr., B. Chu-Kung, G. Walter, and R. Chan, Appl. Phys. Lett. **84**, 4792 (2004).
[7]F. Dixon, M. Feng, N. Holonyak, Jr., Yong Huang, B. Zhang, J. H. Ryou, and R. D. Dupuis, Appl. Phys. Lett. **93**, 021111 (2008).
[8]H. W. Then, C. H. Wu, G. Walter, M. Feng, and N. Holonyak, Jr., Appl. Phys. Lett. **94**, 101114 (2009).
[9]R. Chan, M. Feng, N. Holonyak, Jr., and G. Walter, Appl. Phys. Lett. **86**, 131114 (2005).
[10]M. Feng, N. Holonyak, Jr., A. James, K. Cimino, G. Walter, and R. Chan, Appl. Phys. Lett. **89**, 131504 (2006).
[11]M. Feng, H. W. Then, N. Holonyak, Jr., G. Walter, and A. James, Appl. Phys. Lett. **95**, 033509 (2009).
[12]M. Feng, N. Holonyak, Jr., H. W. Then, and G. Walter, Appl. Phys. Lett. **91**, 053501 (2007).
[13]H. W. Then, M. Feng, and N. Holonyak, Jr., J. Appl. Phys. **107**, 094509 (2010).
[14]L. Zhang and J. P. Leburton, IEEE J. Quantum Electron. **45**, 359 (2009).
[15]B. Faraji, W. Shi, D. L. Pulfrey, and L. Chrostowski, Appl. Phys. Lett. **93**, 143503 (2008).
[16]B. Faraji, D. L. Pulfrey, and L. Chrostowski, Appl. Phys. Lett. **93**, 103509 (2008).
[17]B. Faraji, W. Shi, D. L. Pulfrey, and L. Chrostowski, IEEE J. Sel. Top. Quantum Electron. **15**, 594 (2009).
[18]B. G. Streetman and S. Banerjee, *Solid State Electronic Devices, 6th edition* (Prentice–Hall International, Englewood Cliffs, NJ, 2008).
[19]R. Basu, B. Mukhopadhyay, and P. K. Basu, Semicond. Sci. Technol. **26**, 105014 (2011).
[20]R. Basu, B. Mukhopadhyay, and P. K. Basu, Semicond. Sci. Technol. **27**, 015022 (2012).
[21]A. A. Grinberg and S. Luryi, IEEE Trans. Electron. Devices **40**, 859 (1993).
[22]P. K. Basu, *Theory of Optical Processes in Semiconductors: Bulk and Microstructures* (Oxford University Press, Oxford, UK, 2003).